

# REACTION PATHWAYS AND CATALYST REQUIREMENTS IN THE SYNTHESIS OF ISOBUTANOL FROM CO AND H<sub>2</sub>

Mingting Xu, Brandy L. Stephens, Marcelo J.L. Gines, and Enrique Iglesia  
Department of Chemical Engineering, University of California, Berkeley, CA 94710

## 1. ABSTRACT

The synthesis of isobutanol and methanol from CO/H<sub>2</sub> on K-Cu-Mg-CeO<sub>x</sub> catalysts is inhibited by CO<sub>2</sub>, one of the reaction products. Alcohol coupling reactions show that CO<sub>2</sub> decreases the rates of both alcohol dehydrogenation and base-catalyzed chain growth condensation reactions. Basic site density and reactivity were determined using a <sup>12</sup>CO<sub>2</sub>/<sup>13</sup>CO<sub>2</sub> isotopic transient technique. Addition of K to Cu-Mg-CeO<sub>x</sub> increases both basic site density and strength, but influences weakly the rate of base-catalyzed alcohol coupling reactions. Cu enhances the rates of alcohol dehydrogenation, and Ce increases Cu dispersion and stabilizes high surface area MgO. The cross-coupling reactions of acetaldehyde and <sup>13</sup>C-labeled methanol produce singly-labeled propionaldehyde, suggesting that it forms by the condensation of acetaldehyde and a reactive intermediate derived from methanol. Isobutyraldehyde, a precursor to isobutanol, forms via the condensation of propionaldehyde and reactive C<sub>1</sub> species resulting from methanol. Temperature-programmed surface reaction studies of preadsorbed ethanol have shown that CO decreases the rate of base-catalyzed self-condensation reactions of ethanol to acetone, possibly due to the poisoning of basic and metal sites by the CO<sub>2</sub> formed from CO by water-gas shift or Boudouard reactions.

## 2. INTRODUCTION

Isobutanol is a potential fuel additive and MTBE precursor, but currently available catalysts for the conversion of H<sub>2</sub>/CO mixtures to isobutanol require high temperatures (> 400 °C) and pressures (> 10 MPa) and produce isobutanol with relatively low productivity (< 100 g/kg-cat-h) and selectivity (< 25 mol. %)[1-5]. Significantly higher isobutanol yields and selectivity at reaction conditions attainable in slurry bubble column reactors would improve the efficiency and economics of isobutanol synthesis process.

Our research addresses the design and synthesis of low-temperature (< 350 °C) and low-pressure (< 100 bar) isobutanol synthesis catalysts. K-Cu-Mg-CeO<sub>x</sub> catalysts [6] were chosen for initial studies because they are among the best reported catalysts for low-temperature isobutanol synthesis. The samples were prepared by coprecipitation and incipient wetness methods designed to maximize the dispersion of active components; they were evaluated at 4.5 MPa, 300-360 °C, and a CO/H<sub>2</sub> ratio of 1 in a packed-bed tubular microreactor (CMRU). Reaction pathways for the synthesis of isobutanol and its molecular precursors (ethanol, 1-propanol) were studied by examining the adsorption and surface reactions of alcohols and aldehydes in a gradientless recirculating reactor (RRU) and a temperature-programmed surface reaction (TPSR) apparatus. The role of individual element in multicomponent catalysts was explored by varying the composition of K-Cu-Mg-CeO<sub>x</sub> catalysts.

### 3. CATALYST SYNTHESIS AND CHARACTERIZATION

Cu-Mg-CeO<sub>x</sub> samples were prepared by coprecipitation of mixed nitrate solutions with 2 M KOH and 1 M K<sub>2</sub>CO<sub>3</sub> at 65 °C and with a constant pH of 9 in a computer-controlled well-stirred batch reactor. The resulting solids were filtered, washed thoroughly with distilled water at 60 °C, and dried at 80 °C overnight. Samples were treated in air at 450 °C for 4 h to form the metal oxides. All samples were reduced in flowing H<sub>2</sub> before catalytic experiments. The properties of these mixed metal oxide catalysts are given in Table 1.

**Table 1.** Composition, surface area, basic site density of mixed metal oxides

<sup>a</sup> Sample	<sup>b</sup> S <sub>g</sub> , m <sup>2</sup> /g	<sup>b</sup> Cu, dispersion, %	Exchangeable CO <sub>2</sub> at 300 °C 10 <sup>-6</sup> mol/m <sup>2</sup>	CO <sub>2</sub> desorbed during TPD at T < 300 °C 10 <sup>-6</sup> mol/m <sup>2</sup>
1.2 wt% K-Cu <sub>7.5</sub> Mg <sub>5</sub> CeO <sub>x</sub>	92	5	3.28	0.91
5.3 wt% K-Mg <sub>5</sub> CeO <sub>x</sub>	53	/	---	---
0.1 wt% K-Cu <sub>0.5</sub> Mg <sub>5</sub> CeO <sub>x</sub>	167	23	1.20	0.62
1.1 wt% K-Cu <sub>0.5</sub> Mg <sub>5</sub> CeO <sub>x</sub>	147	14	2.33	0.64
2.6 wt% K-Cu <sub>0.5</sub> Mg <sub>5</sub> CeO <sub>x</sub>	93	7	3.48	0.43

<sup>a</sup> Bulk composition measured by atomic absorption.

<sup>b</sup> Total surface area determined by N<sub>2</sub> BET adsorption at 77 K.

<sup>c</sup> Dispersion calculated from the ratio of surface Cu (determined by N<sub>2</sub>O decomposition at 90 °C [7,8]) to the total number of Cu atoms in the catalyst.

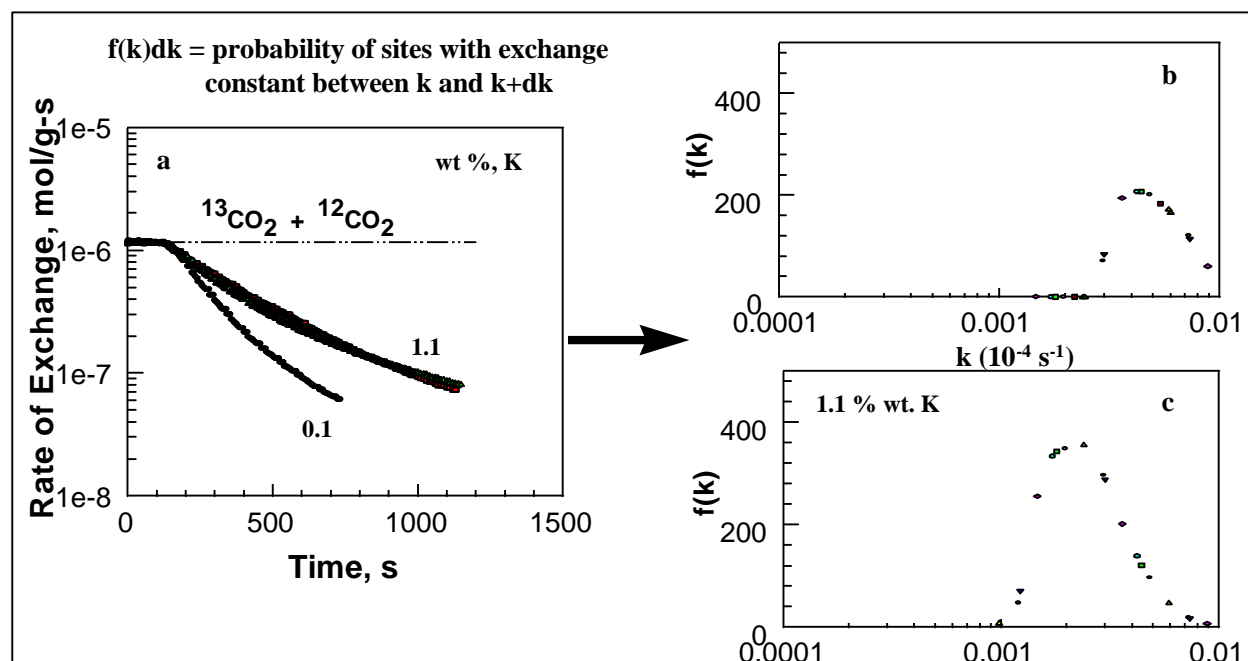


**Figure 1.** Exchange methods probe dynamics on non-uniform surface of K-CuMg<sub>5</sub>CeO<sub>x</sub>.

Cu dispersion decreased with increasing K-loading because of a decrease in MgCeO<sub>x</sub> surface area and possibly also because K-species block surface Cu atoms, resulting in a decrease in the number of exposed surface Cu atoms (Table 1). The density of basic sites was determined using a <sup>13</sup>CO<sub>2</sub>/<sup>12</sup>CO<sub>2</sub> exchange method. This method provides a direct measure of the number of basic

sites “kinetically available” for adsorption and catalytic reactions at reaction conditions. In addition, this technique gives the distribution of reactivity for such basic sites. In this method, a pre-reduced catalyst was exposed to a 0.1 %  $^{13}\text{CO}_2/\text{He}$  stream and after  $^{13}\text{CO}_2$  reached a constant level in the effluent, the flow was switched to 0.1 %  $^{12}\text{CO}_2/\text{He}$ . The relaxation of the  $^{13}\text{CO}_2$  removed from the surface was followed by mass spectrometry. The exchange capacity (Table 1) and dynamics (Figure 1) at reaction temperature were calculated from these data. As a comparison, the basic site densities determined by the conventional temperature-programmed desorption (TPD) of  $\text{CO}_2$  are also listed in Table 1. The TPD experiment consists of adsorbing  $\text{CO}_2$  on the pre-reduced catalyst at room temperature, and while flushing the surface with He to remove gas phase and weakly adsorbed  $\text{CO}_2$ , linearly ramping the temperature, and measuring the desorption profile of  $\text{CO}_2$  by mass spectrometry. This method gives both physically and chemically adsorbed  $\text{CO}_2$ . Nevertheless, the number of basic sites determined from  $\text{CO}_2$  TPD based on the total amount of  $\text{CO}_2$  desorbed below 300 °C is lower than that measured by the  $^{13}\text{CO}_2/^{12}\text{CO}_2$  switch experiment.

The response curves obtained by  $^{13}\text{CO}_2/^{12}\text{CO}_2$  switch experiments on K-promoted  $\text{Cu}_{0.5}\text{Mg}_5\text{CeO}_x$  are shown in Figure 1a. The exchange capacity is determined from the area of the  $^{13}\text{CO}_2$  curve and is reported in Table 1. The local slope in this semi-logarithmic plot reflects exchange dynamics and thus the kinetic behavior of basic sites. The curvature of the semi-logarithmic curve indicates the heterogeneity of surface basic sites since a linear line would be expected of a uniform surface. Short relaxation times (e.g. 0.1 wt % K) reflect short  $\text{CO}_2$  surface lifetimes, high exchange rates, and more weakly titrated basic sites. K increases not only the basic site density in  $\text{Cu}_{0.5}\text{Mg}_5\text{CeO}_x$  (Table 1) but also the strength of basic sites, as shown by the shift in site distribution to lower exchange rate constants (Figure 1b, 1c). The distribution of exchange rate constants (Figures 1b and 1c) were obtained using inverse Laplace transform deconvolution methods [9]. In contrast with  $\text{CO}_2$  temperature-programmed desorption (TPD),  $^{13}\text{CO}_2/^{12}\text{CO}_2$  exchange methods probe the density and reactivity of basic sites at reaction temperatures, without contributions from unreactive carbonates and without disrupting the steady-state surface composition of catalytic solids. As we discuss below, the competitive adsorption of  $\text{CO}_2$  with aldol-coupling precursors on basic sites appears to be one of the hurdles in achieving high isobutanol synthesis rates at low temperatures.

#### **4. ISOBUTANOL SYNTHESIS AT HIGH PRESSURE IN THE CATALYTIC MICROREACTOR UNIT (CMRU)**

A number of low-temperature and low-pressure catalysts have been developed in recent years [6, 10]. Among them, K- $\text{Cu}_{0.5}\text{Mg}_5\text{CeO}_x$  shows one of the highest isobutanol synthesis rates with high alcohol-to-hydrocarbon ratios. Alcohol synthesis rates on K-modified  $\text{Cu}_{0.5}\text{Mg}_5\text{CeO}_x$  catalysts depend strongly on K-concentration. Samples with 1.0-1.5 wt % K-loading give the highest isobutanol synthesis rates. K appears to increase basic site density and strength (see Section 3), a requirement for base-catalyzed chain-growth reactions, and to decrease the density of acid sites, which form dimethylether and hydrocarbons. High K concentrations, however, result in sintering of the metal oxide supports and may also decrease the dispersion or accessibility of Cu crystallites.

The effects of space velocity (SV) on alcohol synthesis rates and selectivity on K-promoted  $\text{Cu}_{0.5}\text{Mg}_5\text{CeO}_x$  are shown in Figure 2. The decrease in CO conversion rate (CO conversion times space velocity) at long residence times reflects the gradual approach to equilibrium for the primary methanol synthesis step, and also the poisoning of methanol-synthesis sites by  $\text{CO}_2$  (one

of the reaction products) as evidenced by the decrease in methanol selectivity. Isobutanol and the other high alcohol selectivities were almost independent of residence time, suggesting that the decrease in methanol selectivity on  $\text{K-Cu}_{0.5}\text{Mg}_5\text{CeO}_x$  was caused exclusively by  $\text{CO}_2$  inhibition of methanol synthesis. Highly dispersed Cu crystallites strongly interacting with  $\text{CeO}_x$  moieties in these samples appear to favor the formation of chemisorbed oxygen species, especially as the concentration of  $\text{CO}_2$  increases with increasing residence time, resulting in a decrease in Cu sites.  $\text{CO}_2$  could also block the basic sites that are required for the base-catalyzed chain-growth reactions leading to isobutanol. The weak dependence of CO conversion and isobutanol selectivity on space velocity suggests that most products are formed near the reactor inlet. The remaining catalyst sections contain  $\text{CO}_2$  concentrations that reversibly inhibit methanol synthesis and chain growth pathways. Methanol and isobutanol productivities reported here are therefore lower bounds, because the observed products arise from a small fraction of the catalyst bed.

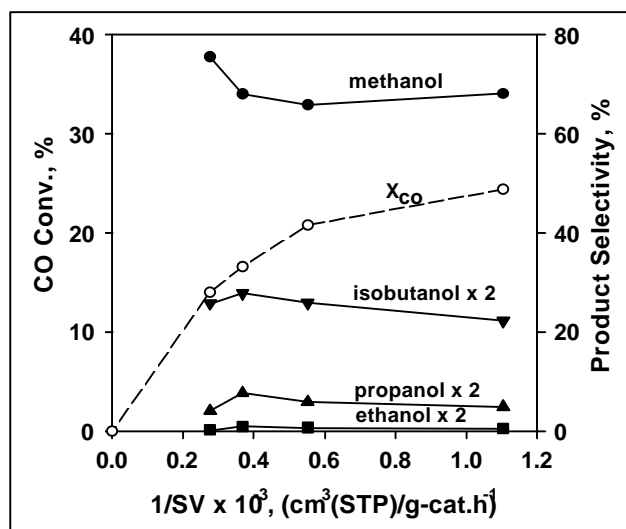


**Figure 2** CO conversion and product selectivities vs. space velocity on  $\text{K-Cu}_{0.5}\text{Mg}_5\text{CeO}_x$ .  $T = 320^\circ\text{C}$ ,  $P = 5.1\text{ MPa}$ ,  $\text{CO}/\text{H}_2 = 1$ .

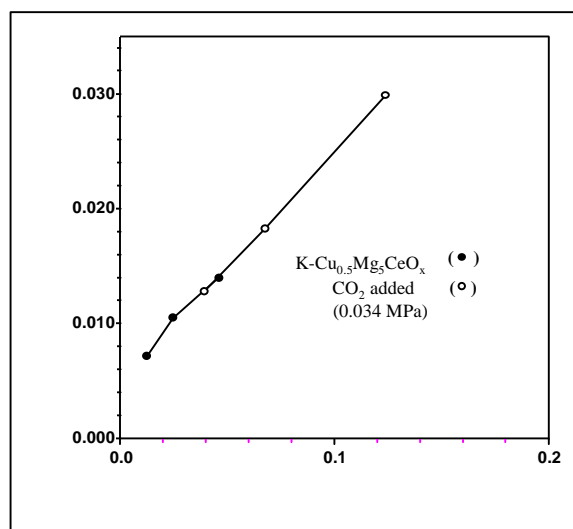


**Figure 3** reciprocal methanol productivity vs. average  $\text{CO}_2$  pressure.  $T = 320^\circ\text{C}$ ,  $P = 4.5\text{ MPa}$ ,  $\text{CO}/\text{H}_2 = 1$ .

The inhibition effect of  $\text{CO}_2$  on methanol productivity on  $\text{K-Cu}_{0.5}\text{Mg}_5\text{CeO}_x$  was confirmed by adding  $\text{CO}_2$  to the  $\text{CO}/\text{H}_2$  feed gas. For example, addition of 0.034 MPa of  $\text{CO}_2$  caused a decrease in methanol productivity from 95.1 to 54.8  $\text{g}/\text{kg-cat.h}$  at a space velocity of 3000  $\text{cm}^3(\text{STP})/\text{g-cat.h}$ . The reciprocal methanol productivity with respect to average  $\text{CO}_2$  pressure on  $\text{K-Cu}_{0.5}\text{Mg}_5\text{CeO}_x$  yields a linear relationship (Figure 3), suggesting a first-order inhibition effect of  $\text{CO}_2$ .  $\text{CO}_2$  pressure is the average of inlet and outlet  $\text{CO}_2$  pressures. From the ordinate intercept the unpoisoned rate of methanol formation can be determined.

As mentioned above, the highly dispersed Cu is more likely to react with  $\text{CO}_2$  resulting in a decrease in Cu sites, and consequently a decrease in methanol productivity. It should be pointed out that low  $\text{CO}_2$  concentrations have positive effects on methanol productivity on a commercial methanol-synthesis catalysts (i.e.,  $\text{Cu}/\text{ZnO}/\text{Al}_2\text{O}_3$ ) [11,12]. The smaller Cu crystallites and higher  $\text{CO}_2$  concentrations in our studies account for the  $\text{CO}_2$  detrimental effects. Methanol-synthesis studies carried out on  $\text{K-Cu}_{7.5}\text{Mg}_5\text{CeO}_x$  showed that methanol productivity on high-Cu  $\text{Mg}_5\text{CeO}_x$  catalysts, i.e., was less affected compared to that on low-Cu catalyst ( $\text{K-Cu}_{0.5}\text{Mg}_5\text{CeO}_x$ ), suggesting that the larger Cu crystallites are more resistant to surface oxidation by  $\text{CO}$ .

## 5. KINETIC STUDIES OF ALCOHOL COUPLING REACTIONS

Ethanol dehydrogenation-coupling reactions were carried out on  $\text{Mg}_5\text{CeO}_x$ ,  $\text{Cu}_{0.5}\text{Mg}_5\text{CeO}_x$  and  $\text{Cu}_{0.5}\text{Mg}_5\text{CeO}_x/\text{K}$  (1 wt %) in a gradientless batch reactor in order to determine the role of Cu, K, and Mg-Ce oxides. Acetaldehyde was the initial product of ethanol reactions on  $\text{Cu}_{0.5}\text{Mg}_5\text{CeO}_x$  and a reactive intermediate in the formation of acetone, n-butyraldehyde, and other oxygenates (Figure 4). Site yields are defined as the ratio of ethanol molecules converted to a given product to the number of Cu atoms. Acetone (from acetaldehyde self-condensation followed by decarboxylation) and n-butyraldehyde (from acetaldehyde self-condensation) were the most abundant products of acetaldehyde coupling (Figures 4 and 5). Methyl-ethyl ketone, 2-pentanone, and ethyl acetate were formed in trace amounts.

The effect of each catalyst component in  $\text{K-Cu}_{0.5}\text{Mg}_5\text{CeO}_x$  was determined by comparing its behavior in ethanol reactions with that of samples without Cu or on K (Table 2). Initial reaction rates were obtained from site yield vs. time plots and normalized using the total surface area of each sample. Initial dehydrogenation rates were low on  $\text{Mg}_5\text{CeO}_x$ ; ethanol conversion reached a maximum value of 7%, which is below the equilibrium conversion (90%). Dehydrogenation rates were much higher on  $\text{Cu}_{0.5}\text{Mg}_5\text{CeO}_x$  and  $\text{Cu}_{0.5}\text{Mg}_5\text{CeO}_x/\text{K}$  (1 wt%) than on  $\text{Mg}_5\text{CeO}_x$ , confirming the predominant role of Cu in the formation of acetaldehyde. K-addition decreased ethanol dehydrogenation rates because of the decrease in Cu dispersion. Aldol coupling reactions were slower on Cu-free catalysts because of the low concentration of acetaldehyde formed. At similar acetaldehyde concentrations, however, K had no detectable effect on the rate of base-catalyzed aldol coupling reactions (Table 2).

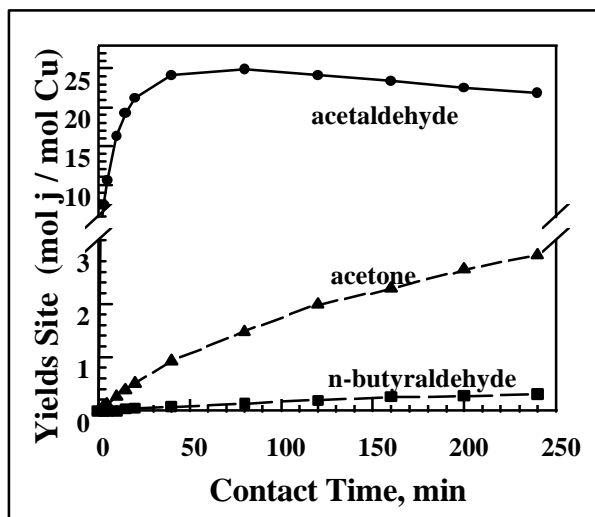


**Figure 4.** Site yields as a function of contact time on  $\text{Cu}_{0.5}\text{Mg}_5\text{CeO}_x$ .

Prior to experiment, the catalyst was reduced in 10 %  $\text{H}_2$  (balance He) at  $350^\circ\text{C}$  for 30 min. The reaction was carried out at  $300^\circ\text{C}$  and 101 kPa. The feed gas composition was  $\text{C}_2\text{H}_5\text{OH}/\text{CH}_4/\text{He} = 4.0/2.7/94.6$  kPa (methane was used as an internal standard).

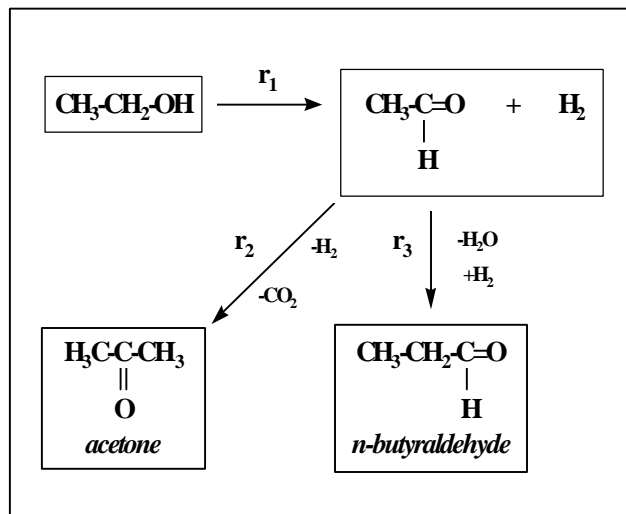


**Figure 5.** Reaction scheme for ethanol reactions.

The effect of  $\text{CO}_2$  on ethanol reactions on  $\text{Cu}_{0.5}\text{Mg}_5\text{CeO}_x/\text{K}$  (1 wt%) was explored by adding 3.5 kPa  $\text{CO}_2$  to ethanol feeds. Both dehydrogenation and coupling reaction rates decreased when  $\text{CO}_2$  was added (Table 3), suggesting that both Cu and basic sites were affected by  $\text{CO}_2$ . These data are consistent with the decrease in both methanol and isobutanol yields as CO conversion increases or  $\text{CO}_2$  is introduced in high-pressure  $\text{CO}/\text{H}_2$  reactions (Figure 2, 3). Titration of basic sites and oxidation of surface Cu atoms by  $\text{CO}_2$  may account for its deleterious effect on catalytic performance.

**Table 2.** Effects of Cu- and K- loading on ethanol consumption and product formation on  $\text{MgCeO}_x$ .

% Cu	% K	Ethanol dehydrogenation ( $r_1$ )	Acetaldehyde to Acetone ( $r_2$ )	Acetaldehyde to Butyraldehyde ( $r_3$ )
0	0	$4.2 \times 10^{-8}$	$.7 \times 10^{-10}$	$6.1 \times 10^{-11}$
0.5	0	$6.4 \times 10^{-7}$	$4.5 \times 10^{-9}$	$3.2 \times 10^{-10}$
0.5	1.1	$3.7 \times 10^{-7}$	$4.2 \times 10^{-9}$	$2.4 \times 10^{-10}$

$r_j$  are expressed in  $\text{mol} / \text{m}^2 \cdot \text{s}$

300°C).

**Table 3.** Effect of  $\text{CO}_2$  on ethanol reaction on  $\text{Cu}_{0.5}\text{Mg}_5\text{CeO}_x/\text{K}$ .

	Ethanol	Ethanol/ $\text{CO}_2$
$r_1$	0.054	0.038
$r_2$	$6.2 \times 10^{-4}$	$2.2 \times 10^{-4}$
$r_3$	$4.6 \times 10^{-5}$	$1.0 \times 10^{-5}$

$r_j$  are expressed in  $\text{mol} / \text{mol Cu} \cdot \text{s}$   
( $\text{C}_2\text{H}_5\text{OH}/\text{CO}_2/\text{CH}_4/\text{He}=4.0/3.3/2.7/91.3$  kPa,

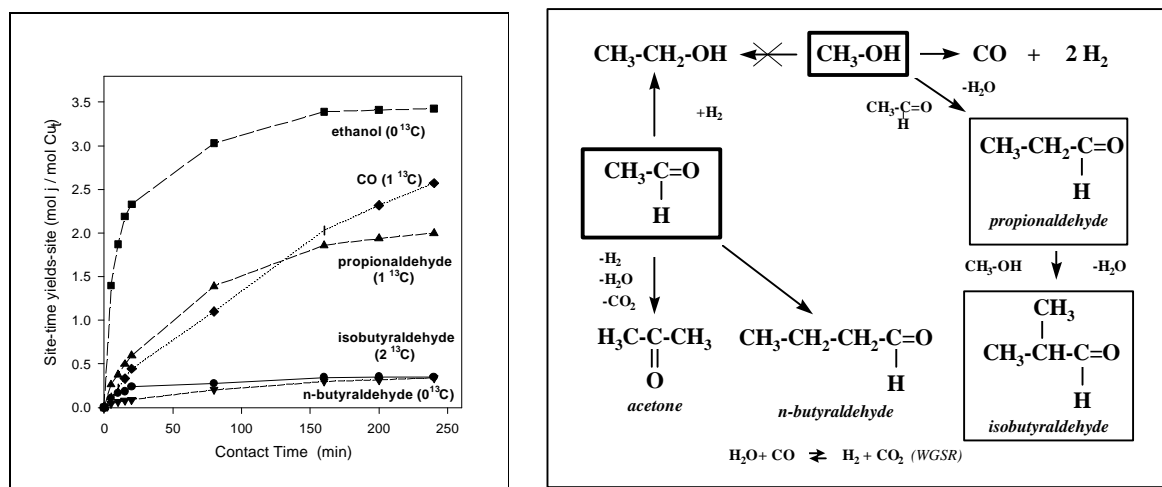


**Figure 6.** Methanol-acetaldehyde reactions. (a) Site yields as a function of contact time on  $\text{Cu}_{0.5}\text{Mg}_5\text{CeO}_x$ . [ $T_r=300^\circ\text{C}$ ,  $P_t=101.3$  kPa,  $P_{\text{methanol}}=8.0$  kPa,  $P_{\text{acetaldehyde}}=4.0$  kPa]; (b) Reaction scheme for methanol-acetaldehyde reactions.

Ethanol is a useful and simple probe molecule to test the metal and basic functions of isobutanol synthesis catalysts. Ethanol reactions, however, lead only to acetone and n-butyraldehyde (precursors to 2-propanol and 1-butanol), neither of which can form isobutanol precursors (e.g. isobutyraldehyde, propionaldehyde) during CO hydrogenation.  $^{13}\text{C}$ -tracer studies of methanol-acetaldehyde cross-coupling reactions were carried out in order to examine reaction pathways leading to chain growth and  $\text{C}_3$  oxygenates. Cross-coupling results on  $\text{Cu}_{0.5}\text{Mg}_5\text{CeO}_x$  are summarized in Figure 6. The initial methanol turnover rate (per mole Cu) from  $^{13}\text{CH}_3\text{OH}-^{12}\text{C}_2\text{H}_4\text{O}$  mixtures was much higher than that of acetaldehyde, but the major products of methanol reactions were  $^{13}\text{CO}$  and  $\text{H}_2$ . The predominant product of acetaldehyde reactions was unlabeled ethanol, formed by acetaldehyde hydrogenation on Cu using the  $\text{H}_2$  formed in methanol decarbonylation reactions. Propionaldehyde contained one  $^{13}\text{C}$  atom, suggesting that it formed by condensation of acetaldehyde with reactive formaldehyde-type intermediates formed during methanol decomposition. Isobutyraldehyde contained two  $^{13}\text{C}$  atoms, suggesting that it formed by condensation of propionaldehyde with formaldehyde.  $\text{CO}_2$  molecules were predominantly labeled and formed from  $^{13}\text{CO}$  via water-gas shift reactions. The remaining products showed no  $^{13}\text{C}$ -enrichment and were formed exclusively via self-condensation reactions of acetaldehyde or ethanol. These products were acetone and n-butyraldehyde. The reaction pathways suggested by these isotopic tracer studies are shown in Figure 6b.

## 6. IDENTIFICATION OF REACTION INTERMEDIATES BY TEMPERATURE-PROGRAMMED SURFACE REACTION (TPSR)

Steady-state catalytic rates reflect the average surface properties of bifunctional and often non-uniform surfaces. Chemical transient methods, such as temperature-programmed surface reaction, complement steady-state studies by varying temporally the surface coverage and temperature and often revealing the kinetic behavior and the storage “capacity” of various reactive pools available on non-uniform surfaces. Our initial TPSR studies have addressed the reactions of ethanol pre-adsorbed on  $\text{Cu}_{0.5}\text{Mg}_5\text{CeO}_x$  samples.

Ethanol appears to adsorb dissociatively on these samples to form surface ethoxide and hydrogen as also reported on ZnO, MgO and Cu [13-16]. The TPSR spectrum of ethanol pre-adsorbed on  $\text{Cu}_{0.5}\text{Mg}_5\text{CeO}_x$  is shown in Figure 7. Unreacted ethanol desorbed at low temperatures by recombination of surface ethoxide with hydrogen. Readsorption effects were ruled out because the desorption spectra shapes were unchanged by variations in carrier gas flow rate, suggesting that evolution rates were controlled by the desorption kinetics.  $\text{H}_2$  desorbed between 100 and 250 °C, leaving ethoxide species on the catalyst surface. The desorption rate and amount increased markedly when Cu was present (Figures 7a, b), as expected from the H-H recombination function provided by Cu and from the mobility of H-atoms on oxides near room temperature. The broad non-symmetric peak of  $\text{H}_2$  suggests the presence of non-uniform desorption sites or multiple sources of H-atoms (Figure 7b). Acetaldehyde formed by additional dehydrogenation of ethoxide species as hydrogen was depleted from the catalyst surface. Some acetaldehyde desorbed unreacted, while the rest underwent coupling reactions to form acetone and trace amounts of acetaldehyde and butyraldehyde (Figure 7).

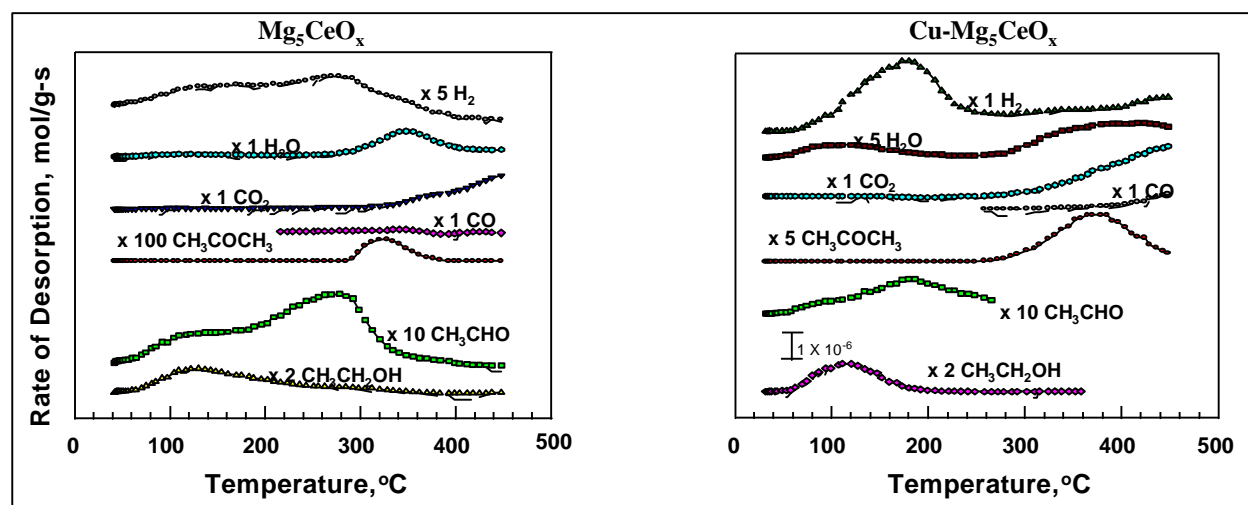
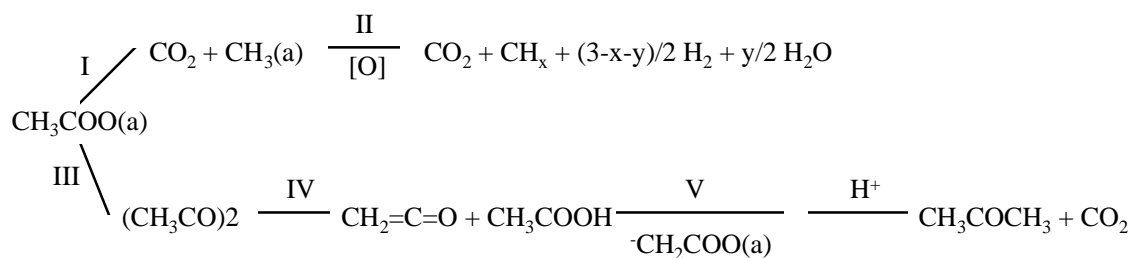


**Figure 7.** Ethanol TPSR on (a)  $\text{Mg}_5\text{CeO}_x$ , (b)  $\text{Cu}_{0.5}\text{Mg}_5\text{CeO}_x$ .

$\text{CO}_2$  and acetone desorbed at similar temperatures (around 300 °C), suggesting that their evolution is limited by the kinetics of decomposition of a common intermediate (Figure 7b). These intermediates are likely to be acetate species formed by nucleophilic attack of carbonyl groups in adsorbed acetaldehyde by electronegative  $\text{O}^{2-}$  species in a reducible metal oxide, such as  $\text{CeO}_2$ . Acetate decomposition also formed  $\text{CO}$ ,  $\text{CO}_2$ ,  $\text{H}_2\text{O}$  and  $\text{H}_2$ , as described by:



**Step I:** Alkyl elimination to produce CO and surface alkyl species [15,17,18].

**Step II:** Alkyl decomposition to form H<sub>2</sub>, H<sub>2</sub>O and carbon on the surface. This surface carbon species can be oxidized by lattice oxygen to produce carbon oxides as proposed by Barbeau et al. on ZnO [15].

**Steps III, IV:** Ketene (CH<sub>2</sub>=C=O), as observed on ZnO by Bowker et al. [18], and on Cu(110) single crystal above 300°C by Madix et al. [17], might form by these two steps.

**Step IV:**  $\text{CH}_2\text{COO(a)}$  surface species, formed by  $\alpha$ -H abstraction, attacks the carbonyl group of CH<sub>2</sub>=C=O, leading to the formation of acetone. Prieto and co-workers proposed a similar mechanism for the formation of acetone from acetic acid on TiQ19].

Since CO is one of the reactants in the syngas-to-isobutanol process, it is important to determine the effect of CO on the base-catalyzed aldol-condensation reactions leading to higher oxygenates. Therefore, ethanol TPSR studies were carried out on Cu<sub>0.5</sub>Mg<sub>5</sub>CeO<sub>x</sub> in the presence of CO. The presence of 5% CO in the carrier gas during reactions of pre-adsorbed ethanol increased the formation of H<sub>2</sub> and CO<sub>2</sub> via water-gas shift reactions above 250 °C, markedly decreased acetone formation, and inhibited the formation of H<sub>2</sub> at low temperatures (Figure 8).

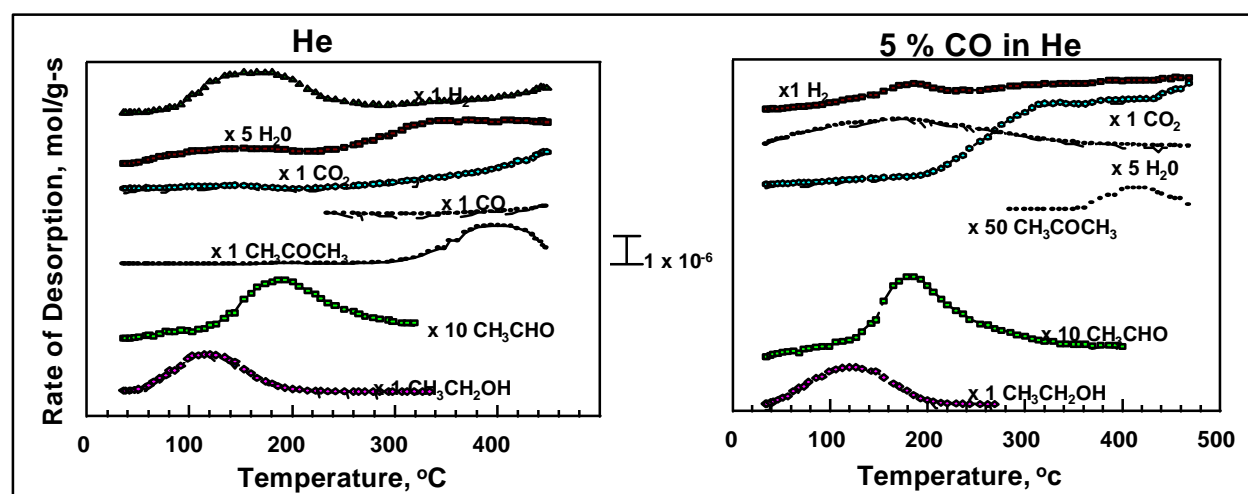


**Figure 8.** Ethanol TPSR on Cu<sub>0.5</sub>Mg<sub>5</sub>CeO<sub>x</sub> in (a) helium flow, (b) 5 % CO in He flow.

The decreased evolution of H<sub>2</sub> is consistent with the loss of Cu sites when CO is present. Cu sites may be blocked by chemisorbed CO or by oxygen atoms formed by interactions of the CO<sub>2</sub> with Cu sites. Temperature-programmed reduction (TPR) experiments of precursor oxides reveal that Cu supported on Mg<sub>5</sub>CeO<sub>x</sub> is more difficult to reduce than that supported on MgO, suggesting a strong interaction between Cu and CeO<sub>2</sub>, which stabilizes Cu<sup>+</sup> ions and results in the high dispersion of Cu on these samples. Cu clusters on Mg<sub>5</sub>CeO<sub>x</sub> appear to be more sensitive to oxidation (by CO<sub>2</sub>) both during catalytic CO hydrogenation and during ethanol TPSR because of their small particle size and the stabilization of Cu<sup>+</sup> by CeO<sub>2</sub> [20,21]. Ethanol TPSR in the presence of CO showed that basic sites responsible for the coupling of adsorbed acetaldehyde species were also blocked by CO<sub>2</sub> (product of water-gas shift or Boudouard reactions). The low



concentration of surface acetaldehyde, precursor to acetone, and the fewer available basic sites are responsible for the marked decrease in acetone production.

## 7. CONCLUSIONS

Strong CO<sub>2</sub> inhibition effect appears to limit methanol and isobutanol synthesis rates at low temperatures on K-Cu-Mg-CeO<sub>x</sub> catalysts. A <sup>13</sup>CO<sub>2</sub>/<sup>12</sup>CO<sub>2</sub> isotopic transient technique has been developed to probe basic site density and strength at typical reaction conditions and to explore the kinetic availability of basic sites during isobutanol synthesis. Isotopic tracer and TPSR studies of alcohol coupling reactions suggest that chain growth occurs by condensation reactions involving the addition of a C species to adsorbed alkoxides.

## 8. ACKNOWLEDGMENTS

This work was supported by Division of Fossil Energy, the United States Department of Energy under Contract Number DE-AC22-94PC94066.

## 9. REFERENCES

1. W. Keim, and W. Falter, *Catal. Lett.* 3 (1989) 59.
2. W. Keim, *D.E. Patent* 3810421 (1988).
3. L. Lietti, P. Forzatti, E. Tronconi, and I. Pasquon, *J. Catal.* 126 (1990) 401.
4. P. Forzatti, E. Tronconi, and I. Pasquon, *Catal. Rev. Sci. Eng.* 33 (1991) 109.
5. A. Sofianos, *Catal. Today* 15 (1990) 119.
6. C.R. Apestequia, S.L. Soled, and S. Mieso U.S. Patent No 5,387,570. Issued Feb. 7, 1995 to Exxon Research & Engineering Co. Florham Pk., N.J.
7. E. Iglesia, and M. Boudart, *J. Catal.* 81 (1983) 204-213.
8. K. Narita, N. Takeyawa, and I. Toyoshima, *React. Kinet. Catal. Lett.* 19 (1982).
9. M. DePontes, G.H. Yokomizo and A.T. Bell, *J. Catal.* 104 (1987) 147-155.
10. J.G. Nunan, P.B. Himmelfarb, R.G. Herman, K. Klier, C.E. Bogdan and G.W. Simmons, *Inorg. Chem.* 28 (1989) 3868-3874.
11. K. Klier, V. Chatikavanu, R.G. Herman, and G.W. Simmons, *J. Catal.* 74 (1982) 343.
12. G. Liu, D. Willcox, M. Garland, and H.H. Kung, *J. Catal.* 90 (1984) 139.
13. M. Bowker and R.J. Madix, *Surf. Sci.* 116 (1982) 549-572.
14. M. Bowker, H. Houghton and K.C. Waugh, *J. Chem. Soc., Faraday Trans. 1* 78 (1982) 2573-2582.
15. J.M. Vohs and M.A. Barteau, *Surf. Sci.* 21 (1989) 590-608.
16. S.L. Parrott, J.W. Rogers, Jr. and J.M. White, *Surf. Sci.* 1 (1978) 443-454.
17. M. Bowker and R.J. Madix, *Appl. Surf. Sci.* 8 (1981) 299-317.
18. M. Bowker, H. Houghton and K.C. Waugh, *J. Catal.* 79 (1983) 431-444.
19. F. Gonzalez, G. Munuera and J.A. Prieto, *J. Chem. Soc., Faraday Trans. I*, 74 (1978) 1517.
20. C. Lamonier, A. Bennani, A. D'uysser, A. Aboukais, and G. Wrobel, *J. Chem. Soc., Faraday Trans.* 92(1) (1996) 131-136.
21. J. Soria, *Solid State Ionics*, 63-65 (1993) 755-761.